Corrosion properties of stainless steel 316 L after energetic nitrogen insertion

L. Escalada [a], J. Lutz [b], S. Mändl [b,*], D. Manova [b], H. Neumann [b], S. Simison [a]

[a] INTEMA, CONICET, Universidad Nacional de Mar del Plata, Argentina
[b] Leibniz-Institut für Oberflächenmodifizierung, Leipzig, Germany

ARTICLE INFO

ABSTRACT

Using a pulse low energy ion implantation with an electronic beam switch operating in the kHz regime, a more efficient nitriding process is possible than with either pulsed plasma immersion ion implantation (PIII) or continuous low energy ion implantation (LEII). Using such an experimental setup, it is shown that the pulse length modulation (PLM) itself produces a slight beneficial effect on the corrosion behaviour of austenitic stainless steel 316 L at 400 °C. However, differences in the diffusion and phase formation exist. For 5% PLM, a lower nitrogen flux resulted in the formation of expanded austenite with a very low lattice expansion, while the highest PLM (40%) led to a reduced layer thickness caused by higher sputtering induced by the increased ion bombardment itself. Nitriding at 400 °C increases the corrosion resistance of 316 L stainless steel for all PLM. The effect is more pronounced for 15 and 30% PLM

© 2011 Elsevier B.V. All rights reserved.

1. Introduction

Nitriding of austenitic stainless steel by energetic ions is nowadays a well-established technology after 15–20 years of developmental research, appearing to be ready for applications in industry [1,2]. The resulting metastable, supersaturated phase is characterised by nitrogen situated on interstitial sites at a concentration between 30 and 40 at.%[3,4].The fast nitrogen diffusion is presently discussed by a trapping/detrapping model resulting in an anisotropic lattice expansion is observed [5,6]. While the very high hardness and wear resistance is well established [7], recent work is still investigating the crystallographic structure of expanded austenite [8,9].

A thermally activated decay into ferritic Fe and CrN is reported with a lifetime between 60 h at 425 °C and less than 2 h at 500 °C [10]. Correlated with this decay, a strong degradation of the corrosion resistance is observed, caused by the precipitation of Cr-N [11], thus depriving the material of mobile Cr atoms from forming a Cr-enriched surface layer. However, even processing at 340–380 °C can lead to a degradation of the corrosion resistance for steel 304 and 316Ti [12]. Furthermore, it has been reported that corrosion resistance of nitrided stainless steel could be altered depending on several process variables, in addition to process time and temperature, [13,14,15,16,17]. Additionally, nitrogen insertion into CoCr alloys with a similarly expanded lattice shows a reduced Cr mobility and a diminished corrosion protection even at lower temperatures without CrN formation [18].

Different methods for nitrogen insertion into steel have been described in the literature, including gas and plasma nitriding [19,20,21],

plasma immersion ion implantation and conventional ion beam implantation [22,23], in addition to broadbeam LEII [24,25]. The latter method can be assumed to be one of the most industry friendly methods due to rather low voltages and a simple experimental setup when certain minimum ion energy is required. Furthermore, modern ion sources can deliver a very high ion flux density across large areas. It has been shown that for sufficiently high current densities, no influence of the current density or the pulse voltage on the diffusion for steel 304 was observed, as long as an exact temperature control of the substrates is accomplished [26]. Otherwise, at lower nitrogen supply, a layer growth limited by nitrogen supply has been observed, together with strong dependencies of the resulting layer thickness on the ion current density and the ion energy [27,28].

However, while the influence of the current density, respective pulse length modulation (PLM) on the diffusion and the formation of the expanded austenite layer on the surface of the implanted steel alloy 304 has recently been published [29], the influence of the PLM on the corrosion resistance, especially the pitting corrosion resistance has not been investigated. In this paper the results of corrosion testing for steel 316 L are presented.

2. Experiment

The samples for these investigations were prepared from austenitic stainless steel (AISI 316 L, corresponding to DIN 1.4404/ X2CrNiMo17.12.2), using a 24 mm diameter rod in form of thin discs with a thickness of 3 mm after cutting. Prior to nitriding the discs were polished to a root mean square surface roughness (R_{rms}) lower than 20 nm. LEII nitriding was carried out using an ECR broad beam ion source with 125 mm beam diameter. The plasma generation frequency was 2.45 GHz with a static magnet field strength of 0.875 T. The nitrogen
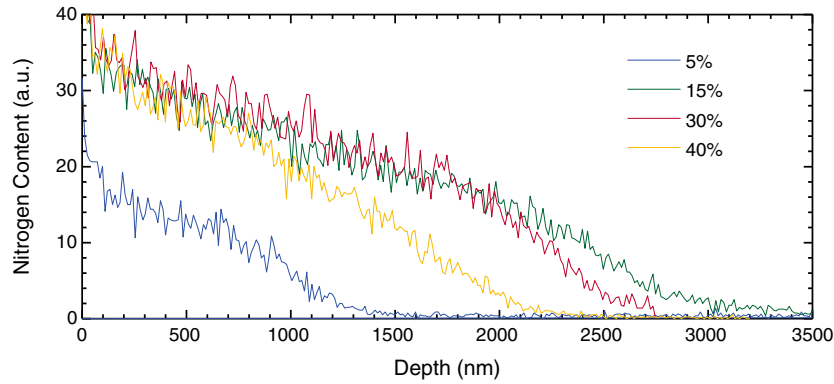
Fig. 1. Variation of nitrogen depth profiles, as determined with SIMS, as function of PLM.

mass flow of 18 sccm resulted in a working pressure of 2×10^{-2} Pa, while the base pressure was always below 7×10^{-4} Pa.

For these experiments the ion beam energy was fixed at 0.8 keV, with the frequency of the beam switch fixed at 1 kHz and the PLM varying between 5 and 40%. At 30% PLM, a current density of 0.45 mA/cm² was measured, translating into an incident nitrogen flux density of 6.5×10^{15} at./cm²s, including corrections for charge exchange and atomic-to-molecular ratios [26,30]. The duration of the experiments was fixed at 90 min while the temperature was controlled to 400 °C, including a fast 9 minute heating phase, by external radiation heating. The temperature was controlled by a feedback loop during the whole experiment. The temperature reproducibility was better than 3–5 °C with negligible influence on the results, as demonstrated before [26].

The phase formation was investigated with X-ray diffraction (XRD) in Bragg–Brentano geometry using Cu K$_\alpha$ radiation (Seifert 3003). The nitrogen depth profiles were measured using time-of-flight secondary ion mass spectrometry (ToF-SIMS). By measuring the crater depth the thickness of the nitrided layers was determined assuming a linear sputter rate with no degrading of the profile edges due to sputter roughening within the crater. The layer thickness was defined by a nitrogen concentration of 3 at.%, which is a reasonable value as nitrogen concentration does not go to zero due to native nitrogen concentration in steel.

Corrosion tests were performed on both the untreated and LEII pulsed treated alloy. Samples were softly polished with alumina suspension in order to eliminate air formed oxides and cleaned in ethanol prior to corrosion test. Electrochemical experiments were conducted at room temperature and atmospheric pressure in a three-electrode cell. A saturated calomel electrode (SCE) was employed as the reference electrode and a platinum spiral wire as the counter electrode. So as to avoid altering ground surface, the samples were pressed against the bottom of the cell and sealed using an O-ring [31]. The resulting working electrode area was 0.41 cm2. A 3.5 wt.% NaCl air saturated solution was used (air was continuously bubbled in the solution in order to get saturation concentration). Localized corrosion resistance was evaluated by cyclic potentiodynamic polarization experiments. The reversal of the potential was done at a fixed, arbitrary chosen current density of 200 μA/cm². The corresponding potential was called E200. During upward scanning, breakdown occurs where the current increases sharply from the passive current level and pits start growing. On reversal of the scan direction, pits repassivate where the current drops back to low values representative of passive dissolution at the protection or repassivation potential (Er). [31,32]. The corrosion potential was monitored for 40 min after which cyclic potentiodynamic anodic curves were carried out at a 1 mV/s sweep rate.

3. Results & discussion

Fig. 1.a shows the nitrogen depth profiles as a function of PLM with values between 5 and 40%. Except for the sample implanted at 5%, nearly identical profiles were obtained, with the surface concentration around 30 at.%. This value is obtained when using the conversion factor established for steel 304, which is estimated to be correct within 5–10% for steel 316 L, too [29]. When looking in detail, the sample implanted at 40% PLM exhibits a thinner layer than the other two, caused by an increased sputter removal at higher current densities. For the sample implanted at 5% PLM, a much reduced nitrogen surface concentration of about 20 at.% is accompanied by a much thinner layer .

The phase formation as elucidated by XRD measurements results only in expanded austenite for all PLM values as can be seen from appearance of peaks on the left side of the both base material peaks at position 39,68° (30% PLM), 40,05° (15% PLM), 40,45° (40% PLM) and 42,18 (5% PLM) for (111) lattice plane and 45,69 ° (30% PLM), 46,53° (15% PLM), 46,61° (40% PLM) and 49,18 (5% PLM) for (200)
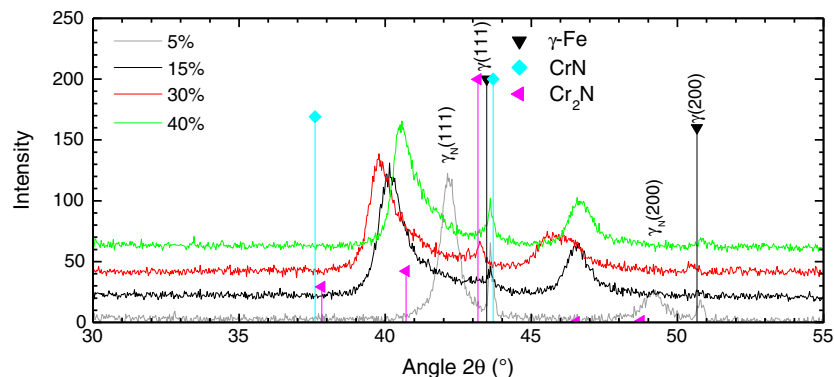

Fig. 2. XRD spectra for samples in the angular range from 30 to 55°.
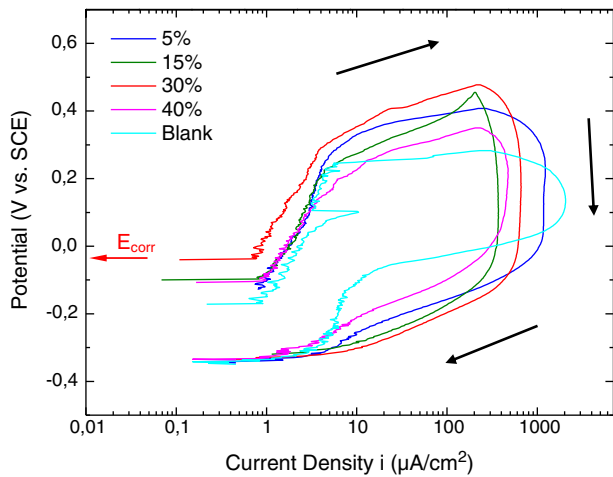
Fig. 3. Polarisation curves for the samples nitrided at various PLM (blank: non treated 316 L).

lattice plane (in Fig. 2, the only position of expanded phase for 5% PLM is indicated). The positions of base material peaks are 43,47° and 50,67 for for (111) and (200) lattice planes, respectively. In particular, no formation of CrN or ferrite was detected (as shown in Fig. 2), which can be expected only for higher temperatures and longer process times. The lattice expansion was calculated using the lattice constant of the base material and expended phase, which were determined from XRD peak positions in the corresponding XRD spectrum. Beyond the initial phase, characterised by 5% PLM, a nearly

constant expansion normal to the surface, is observed with values between 9.6 and 8.6% for the (200) planes normal to the surface and 8.5 to 7.2% for (111) planes normal to the surface, been slightly smaller for the highest PLM value. At 5% nearly identical, low expansion values are found for (111) and (200) planes.

It has to be pointed out that no direct correlation between lattice expansion and nitrogen content exists. The main origin for this behaviour is biaxial stress, resulting in a strain perpendicular to the surface, thus increasing the lattice constant beyond the stress-free value [33]. Accordingly, the sample implanted at 40% PLM should exhibit a lower stress perpendicular to the surface as similar nitrogen surface concentrations are obtained together with a reduced lattice expansion.

The results of the polarization tests are plotted in Fig. 3. Corrosion potentials are shifted up to 150 mV towards more positive values, compared to the untreated specimen. The passive current density is lower and E200 potentials higher for treated samples, indicating that the nitriding produces a beneficial effect on the resistance to localized corrosion of 316 L steel. Although there are not remarkable differences among the nitrided samples the better resistance to localized corrosion is attained for samples with 30 and 15% PLM.

Fig. 4 presents characteristic optical and SEM micrographs of corroded surfaces. The surface attack is inhomogeneous and it is characterised by small pits and etched grain boundaries.

The presented results suggest that the diffusion – and phase formation – is mostly independent of the nitrogen uptake, as long as a minimum effective current density is maintained. As shown before, a minimum value of the current density is necessary to obtain the phase normally known as expanded austenite [29]. For lower PLM values, very small expansions and a much reduced nitrogen depth profile are observed. On the other hand, only slight influence of the nitrogen insertion on the corrosion resistance was found, indicating that for pulsed
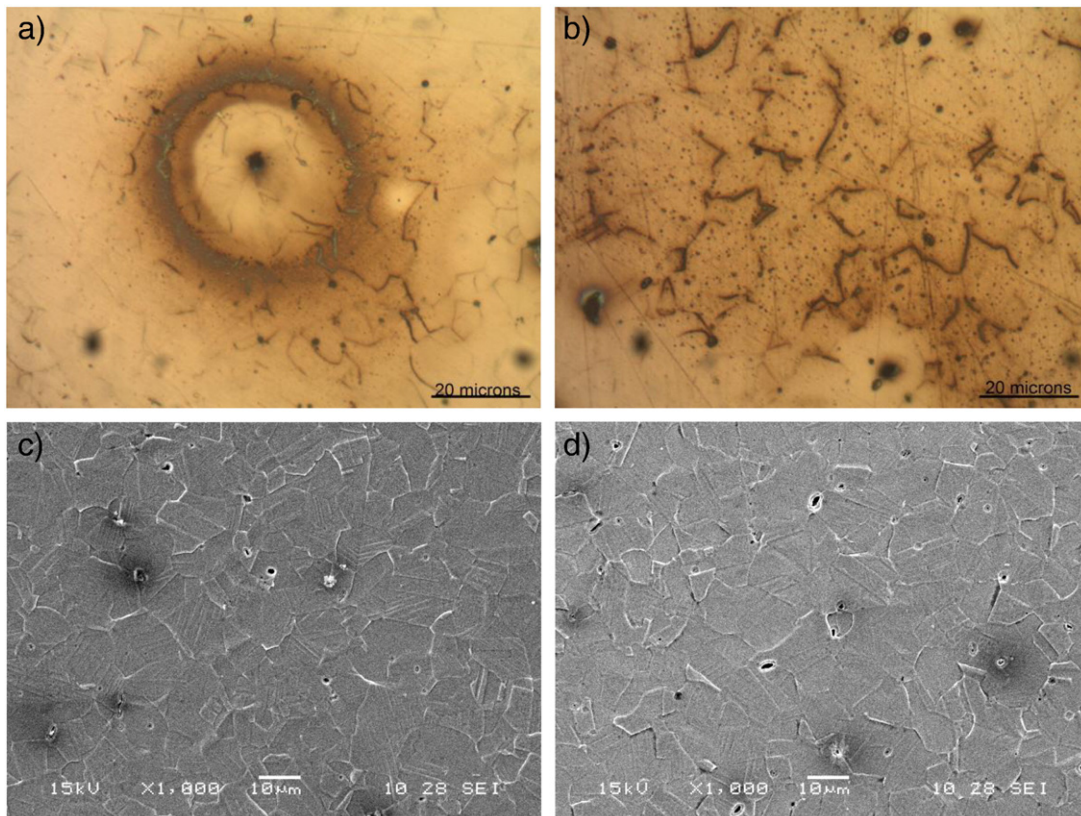

Fig. 4. Surface topography for different samples after corrosion testing: a) 15% PLM, optical viewgraph; b) 30% PLM optical viewgraph; c) 15% PLM SEM viewgraph; d) 30% PLM SEM viewgraph.

LEII, no direct correlation between nitrogen insertion, layer thickness, phase formation and the pitting corrosion exists at 400 °C.

4. Summary & conclusions

316 L austenitic stainless steel was nitrided by LEII using an electronic beam switch, allowing for linear decoupling of ion current density and ion energy. It was shown that nitrogen diffusion is almost independent of nitrogen supply for constant temperature and sufficiently high nitrogen supply. Regarding the nitriding of stainless steel samples, the corrosion resistance shows a small improvement although is not strongly influenced by the pulsed mode, which allows for a faster process and better corrosion resistance at PLM values of around 15%–30%. However, slight variations in the nitrogen surface concentration, ascribed to sputtering effects are not directly reflected in the lattice expansion, indicating that additional effects, e.g. stress may be influential.

Acknowledgements

References

[1] D.L. Williamson, J.A. Davis, P.J. Wilbur, Surf. Coat. Technol. 103/104 (1998) 178.
[2] C. Blawert, B.L. Mordike, Y. Jirásková, O. Schneeweiss, Surf. Coat. Technol. 116/119 (1999) 189.
[3] D.L. Williamson, O. Öztürk, R. Wei, J.P. Wilbur, Surf. Coat. Technol. 65 (1994) 15.
[4] G.A. Collins, R. Hutchings, K.T. Short, J. Tendys, Surf. Coat. Technol. 103/104 (1998) 212.
[5] S. Mändl, B. Rauschenbach, J. Appl. Phys. 88 (2000) 3323.
[6] S. Mändl, Plasma Processes Polym. 4 (2007) 239.
[7] K.H. Lo, C.H. Shek, J.K.L. Lai, Mater. Sci. Eng., R 65 (2009) 39.
[8] A. Martinavičius, G. Abrasonis, W. Möller, C. Templier, J.P. Rivière, A. Declémy, Y. Chumlyakov, J. Appl. Phys. 105 (2009) 093502.
[9] C. Templier, J.C. Stinville, P. Villechaise, P.O. Renault, G. Abrasonis, J.P. Rivière, A. Martinavičius, M. Drouet, Surf. Coat. Technol. 204 (2010) 2551.
[10] T. Bell, Key Eng. Mater. 373/374 (2008) 289.
[11] A. Leyland, D.B. Lewis, P.R. Stevenson, A. Matthews, Surf. Coat. Technol. 62 (1993) 608.
[12] S. Mändl, D. Manova, H. Neumann, M.T. Pham, E. Richter, B. Rauschenbach, Surf. Coat. Technol. 200 (2005) 104.
[13] A. Fossati, F. Borgioli, E. Galvanetto, T. Bacci, Corros. Sci. 48 (2006) 1513.
[14] K.R. Mohan Rao, S. Mukherjee, S.K. Roy, E. Richter, W. Möller, I. Manna, Surf. Coat. Technol. 201 (2007) 4919.
[15] F. Borgioli, A. Fossati, E. Galvanetto, T. Bacci, G. Pradelli, Surf. Coat. Technol. 200 (2006) 5505.
[16] F. Borgioli, A. Fossati, E. Galvanetto, T. Bacci, Surf. Coat. Technol. 200 (2005) 2474.
[17] A. Fossati, F. Borgioli, E. Galvanetto, T. Bacci, Surf. Coat. Technol. 200 (2006) 3511.
[18] J. Lutz, C. Díaz, J.A. García, C. Blawert, S. Mändl, Surf. Coat. Technol. 205 (2011) 3043.
[19] J. Baranowska, Surf. Coat. Technol. 180/181 (2004) 145.
[20] L. Gil, S. Brühl, L. Jiménez, O. Leon, R. Guevara, M.H. Staia, Surf. Coat. Technol. 201 (2006) 4424.
[21] S.P. Brühl, R. Charadia, C. Sanchez, M.H. Staia, Int. J. Mater. Res. 7 (2008) 779.
[22] C. Blawert, H. Kalvelage, B.L. Mordike, G.A. Collins, K.T. Short, Y. Jirásková, O. Schneeweiss, Surf. Coat. Technol. 136 (2001) 181.
[23] R. Wei, J.J. Vajo, J.N. Matossian, P.J. Wilbur, J.A. Davis, D.L. Williamson, G.A. Collins, Surf. Coat. Technol. 83 (1996) 235.
[24] H. Neumann, M. Tartz, F. Scholze, T. Chassé, H. Kersten, H. Leiter, Contrib. Plasma Phys. 47 (2007) 487.
[25] E. Franke, H. Neumann, M. Zeuner, W. Frank, F. Bigl, Surf. Coat. Technol. 97 (1997) 90.
[26] D. Manova, J.W. Gerlach, F. Scholze, S. Mändl, H. Neumann, Surf. Coat. Technol. 204 (2010) 2919.
[27] D.L. Williamson, J.A. Davis, P.J. Wilbur, J.J. Vajo, R. Wei, J.N. Matossian, Nucl. Instrum. Meth. Phys. Res. B 127/128 (1997) 930.
[28] R. Wei, Surf. Coat. Technol. 83 (1996) 218.
[29] D. Manova, F. Scholze, S. Mändl, and H. Neumann, Surf. Coat. Technol. doi:10.1016/j.surfcoat.2011.02.010.
[30] M. Tartz, E. Hartmann, F. Scholze, H. Neumann, F. Bigl, Surf. Coat. Technol. 97 (1997) 504.
[31] S.P. Brühl, R. Charadia, S. Simison, D.G. Lamas, A. Cabo, Surf. Coat. Technol. 204 (2010) 3280.
[32] ASM Handbook, Corrosion, vol. 13A, ASM International, 2003.
[33] D. Manova, J. Lutz, J.W. Gerlach, H. Neumann, S. Mändl, Surf. Coat. Technol. doi:10.1016/j.surfcoat.2010.12.046.